AIP Advances

Gain-switching of 1.55 μm InP-based Qdash lasers grown on Si

Cite as: AIP Advances **12**, 025315 (2022); https://doi.org/10.1063/5.0070129
Submitted: 04 September 2021 • Accepted: 24 January 2022 • Published Online: 10 February 2022

Qi Lin, Ying Xue, Wei Luo, et al.

openaccess

View Online Export Citation CrossMark

AIP Publishing

© 2022 Author(s).

Gain-switching of 1.55 μm InP-based Qdash lasers grown on Si

Cite as: AIP Advances 12, 025315 (2022); doi: 10.1063/5.0070129
Submitted: 4 September 2021 • Accepted: 24 January 2022 •
Published Online: 10 February 2022

View Online Export Citation CrossMark

Qi Lin, Ying Xue, Wei Luo, Jie Huang, Liying Lin, and Kei May Lau[a)]

AFFILIATIONS

Department of Electronics and Computer Engineering, Hong Kong University of Science and Technology, Hong Kong

[a)]**Author to whom correspondence should be addressed:** eekmlau@ust.hk. **Tel.:** (852)23587049. **Fax:** (852) 23581485.

ABSTRACT

Reliable lasers on Si with large bandwidth are desirable for high-performance data communication systems on Si-photonics platforms. Here, we report short optical pulses generated by gain-switched InP-based 1.55 μm quantum dash (Qdash) lasers directly grown on (001) Si. The laser performance and related physical parameters were investigated by carrying out a gain-switching test for lasers on both Si and native InP substrates. The shortest pulses obtained were 217 and 252 ps for the lasers on InP and Si, respectively. By varying the electrical bias and pulse duration systematically, the evolution of the generated optical pulse duration and peak power was studied. The impact of cavity size on the optical pulse was also examined. Parameters were extracted using established equations fitted with our measurement results to gain insight into the underlying physics and correlation with the observed behavior. The obtained results indicate that the pulse width is limited by the low differential gain and strong gain compression of the active material. Our results indicate that Qdash lasers on Si can demonstrate comparable performance to those on a native InP substrate and manifest its potential application in an Si-based photonics chip for optical on-chip communications.

© 2022 Author(s). All article content, except where otherwise noted, is licensed under a Creative Commons Attribution (CC BY) license (http://creativecommons.org/licenses/by/4.0/). https://doi.org/10.1063/5.0070129

The increasing demand for bandwidth places a high requirement on the performance of interconnects in data communications.[1] To address this communication bottleneck, optical interconnects using Si-photonics technology that offer large bandwidth and can be integrated with CMOS electronics are being deployed.[2] In the heart of Si-photonics, III–V lasers on Si have been intensively investigated and reported.[3] III–V lasers can be integrated on a Si substrate by either bonding[4] or direct epitaxy methods.[5] Although bonding-based lasers on Si have demonstrated impressive device performance, lasers on Si realized by direct epitaxy offer an alternative for their potential scalability and high yield.[6,7] However, III–V epitaxy on Si is more challenging due to the large lattice mismatch between III–V materials and Si, thereby leading to reliability concerns in deployment.

To minimize the degradation resulting from mismatch-induced crystal defects, 3D confined quantum structures, including quantum dots (QDs)[8] and quantum dashes (Qdashes),[9] are adopted as the gain media. GaAs-based QD lasers on Si have been demonstrated with a low threshold, high operation temperature, and long lifetime. Many detailed investigations of the physical properties have been made by a few groups.[10,11] However, the emission wavelength is capped at 1.3 μm. Alternatively, InP-based lasers can operate in the O band and C band by tuning the Qdash growth parameters.[12] Recently, our group demonstrated low-threshold, continuous-wave lasing of 1.55 μm InP-based Qdash lasers on Si.[13,14] To further improve the laser performance, theoretical study, experimental investigation, and rigorous analysis of the physical parameters are necessary. Techniques including gain-switching,[15] Q-switching,[16] and mode-locking[17] that are commonly used for short pulse generation are straightforward approaches to investigate the physical mechanisms of III–V lasers. In addition, the generated short pulses can be used for device characterizations in lightwave systems.[12]

In this work, we report gain-switched InP-based 1.55 μm Qdash lasers directly grown on Si. We investigate the influence of the electrical pulse width, electrical bias, and laser cavity size on optical pulse generation and compare the pulses generated by lasers on Si and InP native substrates. The experimental results show shortest pulses of 217 and 252 ps for the lasers on InP and Si, respectively. Subsequently, we use rate equations for the simulation to obtain the

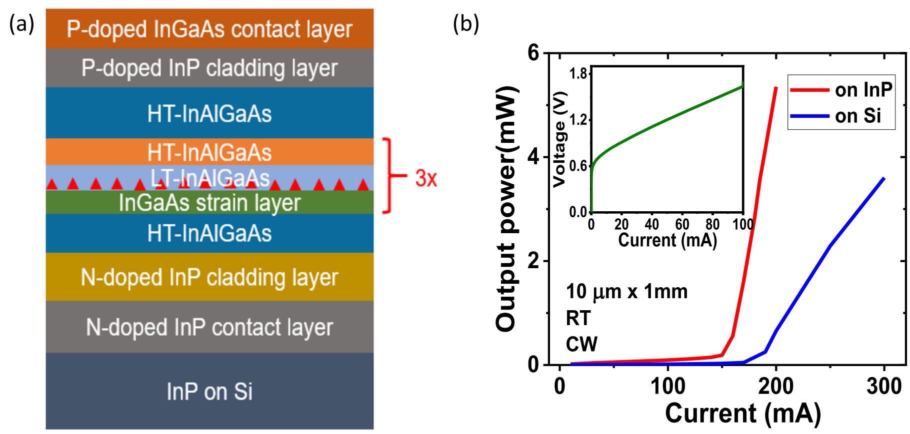

FIG. 1. (a) Growth structure of Qdash lasers on Si and InP native substrates. (b) L–V curve of the lasers on InP and Si used for the gain-switching test.

related parameters and gain insight into the intrinsic performance. Two key parameters, the gain compression factor and the differential gain, are analyzed to provide possible approaches to improve laser performance in the future.

The detailed growth and fabrication information of the Qdash lasers used for our measurement are available in our previous publications.[13,14] Figure 1(a) schematically illustrates the structure of an as-grown Qdash laser on a Si substrate. The threading dislocation density after the growth of the InP buffer is 3.6×10^{8} cm^{-2}. Three layers of Qdashes with a dash-in-well structure are used as the active region. Fabry–Pérot (FP) lasers with different cavity widths and lengths were fabricated with as-cleaved facets on both Si and InP substrates for measurement.

The lasers were placed on a heatsink with a temperature controller and driven under continuous wave (CW) current injection. Light–current (L–I) curves of the lasers on Si and InP substrates are displayed in Fig. 1(b), showing a threshold current of 150 mA on InP and 175 mA on Si. A turn-on voltage of around 0.7 V was measured for the lasers, as shown in the inset of Fig. 1(b).

Figure 2 shows the experimental setup of the gain-switching measurement on our FP lasers. The input electrical signal from a pulse generator was injected into the lasers. Then, the output optical pulse generated by the laser was collected by a lensed fiber, detected by a high-speed photodetector, and finally observed on an oscilloscope.

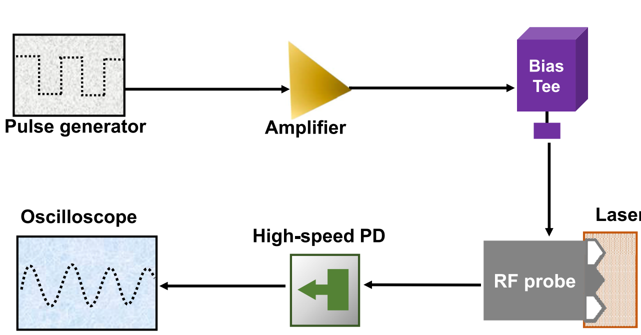

FIG. 2. Experimental setup of the gain-switching measurement on our FP lasers.

The output pulse widths measured under various electrical biases from 3.2 to 4.4 V are shown in Fig. 3(a). Note that the electrical bias is the voltage directly applied to the bias TEE but not to the lasers. With increasing electrical bias, the optical pulse width first decreases until a second relaxation appears[18] and then increases due to excessive carrier injection. For the optical peak intensity, when the electrical pulse width increases, as shown in Fig. 3(b), the optical peak intensity first increases and then levels.[19] The optical pulse width increases with the increase in the electrical pulse width because a long electrical pulse can provide surplus carrier injection [Fig. 3(c)]. However, too narrow an electrical pulse would inversely broaden the optical pulse due to insufficient carriers to switch on the laser, as shown in Fig. 4(a). To achieve a shorter optical pulse width, a shorter cavity length can be adopted with the reduced photon lifetime,[20] as presented in Fig. 4(b). A laser with a 1 mm cavity length generated narrower pulses compared with a laser with a 1.2 mm length under the same measurement conditions and with the same width. Similarly, a narrower cavity can further shorten the optical pulse duration because of the tighter optical confinement in the active layer.

The shortest pulses from the lasers on InP and Si, as shown in Fig. 5, were measured under a bias of 3.8 and 4.3 V, respectively. The difference in the electrical bias on InP and Si is caused by their different threshold voltages. Three parameters of the optical pulse, the rise time, fall time and pulse width, are extracted by a Gaussian fitting. The rise time of the shortest optical pulses are around 97 ps for the lasers on InP and 83 ps for the lasers on Si, while their longer fall times are around 102 and 105 ps, respectively. With the electrical pulse width of 0.63 ns, the shortest laser on Si demonstrates an optical pulse width of 252 ps, which is slightly higher than the 217 ps measured from the lasers on InP. The pulse repetition rate was about 500 MHz, a typical value of gain-switched pulses.[21] The comparable pulse widths measured from the lasers on Si and InP demonstrate similar quality of the Qdashes grown on the two substrates. The pulse durations of our 1.55 μm Qdash lasers grown on Si by metal organic chemical vapor deposition (MOCVD) are somewhat longer than those reported for 1.3 μm QD lasers grown on Si

© Author(s) 2022

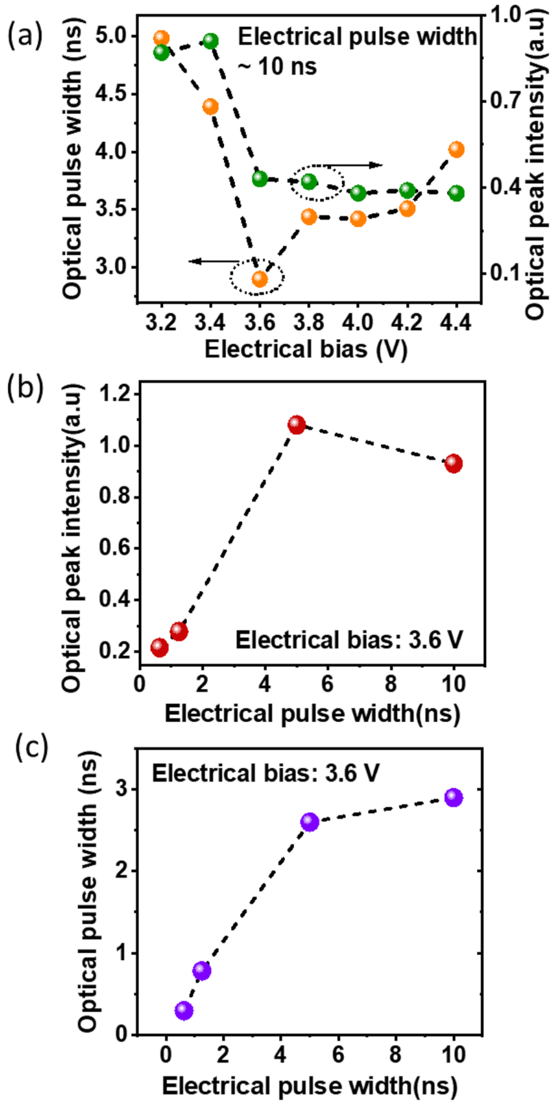

FIG. 3. (a) Electrical bias plotted as a function of the optical pulse width and peak pulse intensity. (b) Relationship of the electrical pulse width and optical peak intensity. (c) Optical pulse duration.

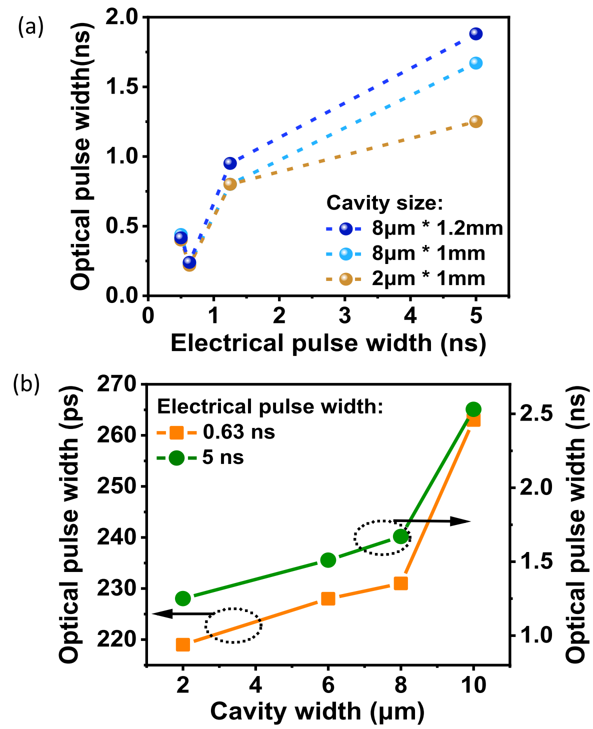

FIG. 4. (a) Evolution of the optical pulse width of three lasers with various dimensions (width × length) at different electrical pulse widths. (b) Influence of cavity width on the optical pulse duration at two different electrical pulse widths of 0.63 and 5 ns.

by molecular beam epitaxy (MBE)[22] but much shorter than that of 1.55 μm quantum well (QW) lasers on Si.[23] The small performance gap between our InP-based Qdash lasers and the well-established GaAs-based QD lasers shows the promise of the InP-based Qdash laser on Si for application in communications, considering future improvement of the buffer and active region. The shorter pulses generated by the Qdash lasers when compared with those from the QW lasers can be attributed to the higher gain in Qdashes.

To determine the limit of the pulse width and point out directions for further improvement, it is necessary to extract and analyze the intrinsic parameters of the 1.55 μm Qdash lasers grown on Si. Several physical mechanisms are expected to be related to the pulse duration: the differential gain determined by the hole spreading in the valence band,[24] the carrier capture effect in the Qdash active region,[25,26] and the stimulated emission rate as affected by the relaxation between the quantized energy states in the Qdashes.[27] To evaluate the impact of these mechanisms and thereby gain insight into the potential performance improvement of the Qdash lasers on Si, key parameters, such as the differential gain and the gain compression factor,[28] need to be calculated first. The rate equations[29] are used to extract the parameters as follows:

$$\frac{dN}{dt} = \frac{I}{qV} - G(N - N_t)S - \frac{N}{\tau_n}, \tag{1}$$

$$\frac{dS}{dt} = G\Gamma(N - N_t)S - \frac{S}{\tau_p} + \frac{\beta \Gamma N}{\tau_n}, \tag{2}$$

where N is the carrier density, S is the photon density, I is the injection current, N_t is the transparent carrier density, τ_n represents the carrier lifetime, Γ is the mode confinement factor, τ_p is the cavity photon lifetime, and β is the fraction of spontaneous emission in the lasing mode. The gain (G) can also be expressed as

$$G = \frac{g_0}{1 + \epsilon S},$$

© Author(s) 2022

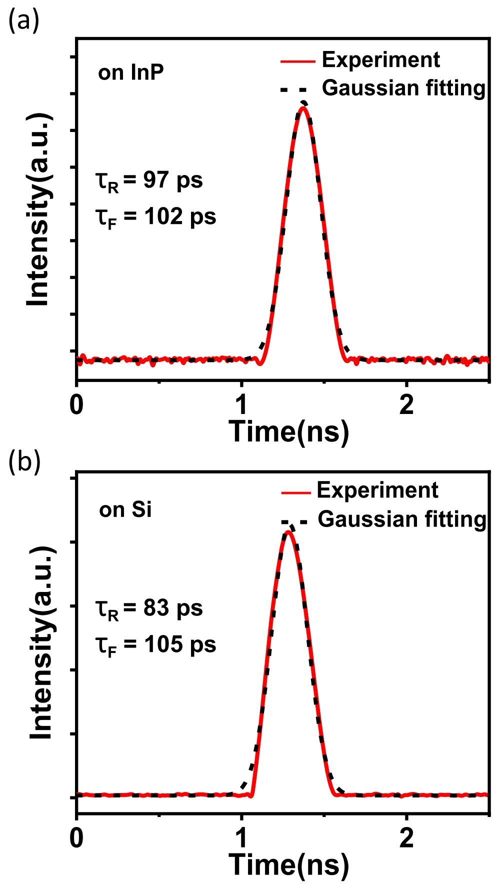

FIG. 5. With the electrical pulse width of 0.63 ns, (a) the shortest laser on InP has a pulse duration of 217 ps at 3.8 V electrical bias and (b) the shortest laser on Si has a pulse duration of 252 ps at 4.3 V electrical bias.

where g_0 is the differential gain and ϵ is the gain compression. The gain model presented is mainly for the following investigation of two key parameters, differential gain and gain compression.

The general evaluation of the rising time τ_r can be calculated through the photon density and the peak carrier density N_p, as shown below; S and $N_p - N_t$ are large enough due to the stimulated emission,[21] and the final term in (2) can be neglected,

$$\frac{1}{S}\frac{dS}{dt} = g_0\Gamma(N_p - N_t) = \frac{1}{\tau_r}. \tag{3}$$

To obtain more information about the dynamic response, small-signal analysis[30] is applied in the rate equation to calculate the modulation bandwidth (f_b) as shown below. The modulation bandwidth could also be a predictor to the generated pulse duration[31] despite their complex relationship. The large differential gain and small gain compression could improve the bandwidth for small signals and shorten the pulse width of the large signal,

$${f_b}^2 = \left(\frac{\omega}{2\pi}\right)^2 = \frac{g_0 v_g S_0}{4\pi^2\tau_p}. \tag{4}$$

Based on the relationships provided in (3) and (4), we obtain a semi-empirical method of decreasing the rising time or pulse duration by changing other related parameters.

Using Eqs. (1) and (2), we conducted a simulation to fit the measured optical pulse. Figure 6(a) shows the simulated and experimental pulses of the gain-switching lasers on InP and Si. The simulation results agree well with the experimental results. In the simulation, different square-wave pulses with a bias of 3.8 V for the laser on InP and 4.3 V for the laser on Si were used to simulate a realistic input electrical signal. To evaluate the accuracy of the fitting, three related parameters were extracted: the pulse duration $\Delta\tau$, rise time τ_r, and fall time τ_f. The simulated $\Delta\tau$, τ_r, and τ_f are 222, 92, and 105 ps, respectively, for the laser on InP, and 246, 84, and 116 ps, respectively, for the laser on Si. These three parameters obtained through the simulation match well with the experimental results.

As shown in Table I, based on the cavity size, optical loss, group velocity, and other commonly used parameters found in the literature,[15,21,32,33] the approximate ranges of the key parameters were determined. Based on the range provided, the transparent carrier density, photon and carrier lifetime, differential gain, and compression factor could be calculated by fitting with the experimental data, as also shown in Table I. The calculated facet reflectivity and the optical loss are similar to the values obtained from experimental measurement and used for our previous analysis,[13,34] which

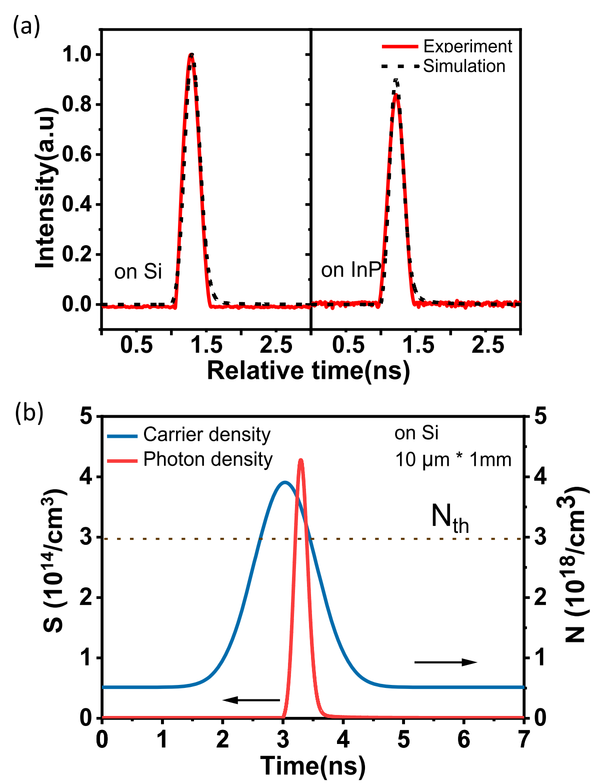

FIG. 6. (a) Simulated and measured gain-switching pulse of the lasers on InP and Si, respectively. (b) Simulated N and S of the laser on Si indicating the dynamic relationship between carriers and photons.

© Author(s) 2022

TABLE I. Parameters of lasers on InP and Si used during simulation.

	Cavity size L × W = 1 mm × 10 μm Optical loss α_i = 15 cm−1 Group velocity v_g = 8.5 × 107 m/s		Facet reflectivity $R_1 = R_2$ = 39% Confinement factor Γ = 0.35 Spontaneous emission coupling factor $\beta = 10^{-4}$		
	Transparent carrier density N_t (cm^{-3})	Carrier lifetime τ_n (ns)	Photon lifetime τ_p (ps)	Differential gain g_0 (cm^3/s)	Gain compression ε (cm^3)
On InP	1×10^{18}	0.5	2.1	5.8×10^{-8}	1×10^{-16}
On Si	1.85×10^{18}	0.7	4.9	6.3×10^{-8}	8×10^{-16}

shows the soundness of the semi-empirical model. The lower transparent carrier density of the lasers on InP leads to lower threshold currents, as proved by the *L–I* measurement. The photon lifetime is comparable due to the same cavity length and reflectivity of the lasers on the Si and InP substrate. The slight difference between them is due to the mismatch induced defects in the lasers on Si. However, the relatively high density of dislocations and lower activation energy of the lasers on the Si substrate result in a larger τ_n and τ_p for the Qdash lasers on Si compared with those on the native InP substrates, leading to a longer pulse of the lasers on Si. The differential gain and gain compression are two critical parameters related to dynamic performance. The differential gain of the laser can affect the rise time of the generated optical pulse, as shown in Eq. (3). To enhance the differential gain, the Al composition can be further tuned for a reduced carrier leakage to continuum states realized by the higher barrier. Meanwhile, the high gain compression factor of 8×10^{-16} cm^3 on Si is comparable to that of GaAs-based QD lasers on Si.[20] The gain compression of the laser on Si is larger than that of the laser on InP, which indicates that high gain compression would broaden the pulse duration and increase the falling time.[22] A high-reflection coating and more stacking of Qdashes can further shorten the generated optical pulses with a smaller gain compression. Increasing the hole population in the p-doped active region has also been proposed in the growth structure to shorten the optical pulse width through faster capture and shorter relaxation times.[35,36]

From the simulated evolution of N and S for the laser on Si shown in Fig. 6(b), the dynamic relationship between the carriers and photons can be revealed. The simulation results show that the photons will increase rapidly with the current injection after the carriers reaches the threshold carrier density N_{th}. During the generation of the pulse, the stimulated emission rapidly depletes free carriers with the change of dS/dt, and then the carrier density is pulled down below the threshold density. The relationship between carrier density and photon density confirms the reliability of the gain switching measurement.

In conclusion, we presented experimental results and a semi-empirical study of gain-switched 1.55 μm Qdash lasers grown on Si and InP. The shortest measured pulse widths of lasers on Si and native InP substrates were 217 and 252 ps, respectively. By varying the electrical bias and pulse duration systematically, the trends of the optical pulse duration and peak power were revealed. The impact of cavity size was also investigated for a shorter pulse. Rate equations were used to calculate the parameters of the shortest experimental pulses and, thus, obtain insight into the lasers' intrinsic performance. Long carrier and photon lifetime, especially low differential gain and strong gain compression, can limit the dynamic performance of the Qdash lasers. Tuning of the Al composition is proposed to increase the differential gain with a higher barrier. A high-reflection coating and more stacking of Qdashes can accomplish lower gain compression and result in a shorter pulse duration. The p-doping of the active region could increase the hole concentration and thereby further shorten the optical pulse duration by increasing the capture and relaxation rates. These results guide future optimization of high-performance 1.55 μm Qdash lasers grown on Si for long-haul communications in Si-photonics.

This work was supported by the Research Grants Council, University Grants Committee (Grant Nos. 16245216 and 16213420) and the Innovation and Technology Fund (Grant No. ITS/273/16FP). The authors thank the NFF (Nanosystem Fabrication Facility) and MCPF (Material Charaterization & Preparation Facility) of HKUST (Hong Kong University of Science and Technology) for technical support. Valuable discussions with Professor Hon Ki Tsang are also acknowledged.

AUTHOR DECLARATIONS

Conflict of Interest

The authors have no conflicts to disclose.

Author Contributions

Q.L. and Y.X. contributed equally to this work.

DATA AVAILABILITY

The data that support the findings of this study are available from the corresponding author upon reasonable request.

REFERENCES

[1] C. Kachris and I. Tomkos, IEEE Commun. Surv. Tutorials **14**(4), 1021–1036 (2012).
[2] M. A. Taubenblatt, J. Lightwave Technol. **30**(4), 448–457 (2011).
[3] J. Richard, P. Doussiere, J. B. Driscoll, W. Lin, H. Yu, Y. Akulova, T. Komljenovic, and J. E. Bowers, IEEE Nanotechnol. Mag. **13**(2), 17–26 (2019).

© Author(s) 2022

[4] G. Roelkens, J. V. Campenhout, J. Brouckaert, D. V. Thourhout, R. Baets, P. R. Romeo, P. Regreny, A. Kazmierczak *et al.*, Mater. Today **10**(7–8), 36–43 (2007).
[5] Y. Wan, Z. Zhang, R. Chao, J. Norman, D. Jung, C. Shang, Q. Li, M. J. Kennedy, D. Liang, C. Zhang, J. Shi, A. C. Gossard, K. M. Lau, and J. E. Bowers, Opt. Express **25**(22), 27715 (2017).
[6] B. Shi, S. Zhu, Q. Li, Y. Wan, E. L. Hu, and K. M. Lau, ACS Photonics **4**(2), 204–210 (2017).
[7] Y. Wan, J. Norman, Q. Li, M. J. Kennedy, D. Liang, C. Zhang, D. Huang, Z. Zhang, A. Y. Liu, A. Torres, D. Jung, A. C. Gossard, E. L. Hu, K. M. Lau, and J. E. Bowers, Optica **4**(8), 940 (2017).
[8] Y. Wan, C. Shang, J. Norman, B. Shi, Q. Li, N. Collins, M. Dumont, K. M. Lau, A. C. Gossard, and J. E. Bowers, IEEE J. Sel. Top. Quantum Electron. **26**(2), 1900409 (2020).
[9] Y. Xue, Y. Wang, W. Luo, J. Huang, L. Lin, H. K. Tsang, and K. M. Lau, Appl. Phys. Lett. **118**(14), 141101 (2021).
[10] A. Lee, Q. Jiang, M. Tang, A. Seeds, and H. Liu, Opt. Express **20**(20), 22181–22187 (2012).
[11] J. Wu, Q. Jiang, S. Chen, M. Tang, Y. I. Mazur, Y. Maidaniuk, M. Benamara, M. P. Semtsiv, W. T. Masselink, K. A. Sablon, G. J. Salamo, and H. Liu, ACS Photonics **3**(5), 749–753 (2016).
[12] W. Luo, Y. Xue, B. Shi, S. Zhu, X. Dong, and K. M. Lau, Appl. Phys. Lett. **116**(14), 142106 (2020).
[13] Y. Xue, W. Luo, S. Zhu, L. Lin, B. Shi, and K. M. Lau, Opt. Express **28**(12), 18172–18179 (2020).
[14] W. Luo, Y. Xue, J. Huang, L. Lin, B. Shi, and K. M. Lau, Photonics Res. **8**(12), 1888–1894 (2020).
[15] B. S. Ryvkin, E. A. Avrutin, and J. T. Kostamovaara, Semicond. Sci. Technol. **26**(4), 045010 (2011).
[16] Y. Chen, G. Jiang, S. Chen, Z. Guo, X. Yu, C. Zhao, H. Zhang, Q. Bao, S. Wen, D. Tang, and D. Fan, Opt. Express **23**(10), 12823–12833 (2015).
[17] Z.-H. Wang, W.-Q. Wei, Q. Feng, T. Wang, and J.-J. Zhang, Opt. Express **29**(2), 674–683 (2021).
[18] P. P. Vasil'ev, I. H. White, and J. Gowar, Rep. Prog. Phys. **63**(12), 1997 (2000).
[19] Y. Xue, X. Wu, W. Luo, S. Zhu, H. K. Tsang, and K. M. Lau, in *IEEE Photonics Conference (IPC)* (IEEE, 2019), pp. 1–2.
[20] H.-F. Liu, M. Fukazawa, Y. Kawai, and T. Kamiya, IEEE J. Quantum Electron. **25**(6), 1417–1425 (1989).
[21] P. Vasil'ev, *Ultrafast Diode Lasers: Fundamentals and Applications* (Artech House, Boston, MA, 1995).
[22] C. Hantschmann, P. P. Vasil'ev, S. Chen, M. Liao, A. J. Seeds *et al.*, J. Lightwave Technol. **36**(18), 3837–3842 (2018).
[23] B. Shi, S. Pinna, H. Zhao, S. Zhu, and J. Klamkin, Phys. Status Solidi A **218**(3), 2000374 (2021).
[24] D. G. Deppe, H. Huang, and O. B. Shchekin, IEEE J. Quantum Electron. **38**(12), 1587–1593 (2002).
[25] A. V. Uskov, Y. Boucher, J. Le Bihan, and J. McInerney, Appl. Phys. Lett. **73**(11), 1499–1501 (1998).
[26] M. Ishida, N. Hatori, T. Akiyama, K. Otsubo, Y. Nakata, H. Ebe, M. Sugawara, and Y. Arakawa, Appl. Phys. Lett. **85**(18), 4145–4147 (2004).
[27] A. Markus and A. Fiore, Phys. Status Solidi A **201**(2), 338–344 (2004).
[28] A. Fiore and A. Markus, IEEE J. Quantum Electron. **43**(4), 287–294 (2007).
[29] J. Bowers, B. Hemenway, A. Gnauck, and D. Wilt, IEEE J. Quantum Electron. **22**(6), 833–844 (1986).
[30] R. Nagarajan, M. Ishikawa, T. Fukushima, R. S. Geels, and J. E. Bowers, IEEE J. Quantum Electron. **28**(10), 1990–2008 (1992).
[31] D. Gready, G. Eisenstein, M. Gioannini, I. Montrosset, D. Arsenijevic *et al.*, Appl. Phys. Lett. **102**(10), 101107 (2013).
[32] P. Paulus, R. Langenhorst, and D. Jager, IEEE J. Quantum Electron. **24**(8), 1519–1523 (1988).
[33] P. Downey, J. Bowers, R. Tucker, and E. Agyekum, IEEE J. Quantum Electron. **23**(6), 1039–1047 (1987).
[34] Z. Li, S. Shutts, Y. Xue, W. Luo, K. M. Lau, and P. M. Smowton, Appl. Phys. Lett. **118**(13), 131101 (2021).
[35] J. Siegert, S. Marcinkevicius, and Q. X. Zhao, Phys. Rev. B **72**(8), 085316 (2005).
[36] K. W. Sun, A. Kechiantz, B. C. Lee, and C. P. Lee, Appl. Phys. Lett. **88**(16), 163117 (2006).

© Author(s) 2022